Indirect tensile versus two-point bending fatigue testing

Article *in* ICE Proceedings Transport · January 2008

DOI: 10.1680/tran.2008.161.4.207

CITATIONS
41

READS
2,197

4 authors, including:

Cesare Sangiorgi
University of Bologna
122 PUBLICATIONS **1,949** CITATIONS
SEE PROFILE

Gordon D. Airey
University of Nottingham
276 PUBLICATIONS **8,148** CITATIONS
SEE PROFILE

Andrew Collop
De Montfort University
106 PUBLICATIONS **3,603** CITATIONS
SEE PROFILE

Proceedings of the Institution of Civil Engineers
Transport 161
November 2008 Issue TR4
Pages 207–220
doi: 10.1680/tran.2008.161.4.207
Paper 700003
Received 22/01/2007
Accepted 12/03/2008
Keywords:
bitumen & tar/fatigue/strength & testing of materials

Andrea Cocurullo
Researcher, University of Bologna, Italy

Gordon D. Airey
Professor, Nottingham Transportation Engineering Centre, University of Nottingham, UK

Andrew C. Collop
Professor, Nottingham Transportation Engineering Centre, University of Nottingham, UK

Cesare Sangiorgi
Research Fellow, University of Bologna, Italy

Indirect tensile versus two-point bending fatigue testing

A. Cocurullo PhD, G. D. Airey PhD, A. C. Collop PhD and C. Sangiorgi PhD

This paper describes a comparison between an indirect tensile fatigue method and the currently preferred European standard two-point bending, trapezoidal fatigue test. A study was undertaken using both tests to determine the fatigue properties of a standard UK asphalt mixture at two temperatures of 10 and 30 °C. The fatigue life, in addition to using the traditional 90% reduction in initial stiffness, was also computed using a fatigue failure point based on the transition between the quasi-stationary phase (associated with a uniform stiffness decrease and the development of micro-cracks) and the failure phase (associated with localised crack propagation). This fatigue failure point, determined by taking the peak of the product of loading cycles and stiffness versus loading cycles, was also converted into an alternative form used to determine the fatigue failure point for the indirect tensile fatigue test. Separate fatigue relationships were produced for the four combinations of test method and temperature based on the phenomenological initial tensile strain versus fatigue life relationship. Although the indirect tensile fatigue test produced shorter fatigue lives compared to the two-point bending fatigue test, it was also possible to combine all four fatigue relationships to produce one unique fatigue function for the 20 mm dense bitumen macadam asphalt mixture.

1. INTRODUCTION

Fatigue is one of the main failure modes of a pavement structure which results in degradation of the bound pavement materials and finally the pavement structure. Two phases of the degradation process occur during fatigue cracking. The first phase corresponds to degradation resulting from damage that is uniformly distributed throughout the material. This phase is manifested by the initiation and propagation of a network of 'micro-cracks' which results in a decrease in the macroscopic rigidity (stiffness modulus) of the material. The second phase starts with the coalescence of these 'micro-cracks' and the appearance of 'macro-cracks' which propagate within the material. These two phases are typically referred to as crack initiation and crack propagation and are usually modelled separately within different theoretical frameworks.

Fatigue behaviour tends to be very sensitive to boundary and loading conditions resulting in a scatter of fatigue results and making the general interpretation relatively complex. In addition, various testing geometries and loading conditions, with their own advantages and disadvantages, are currently used to quantify the fatigue life of an asphalt mixture.[1] The European Committee for Standardization (CEN) is moving towards a single asphalt mixture fatigue test to promote technical harmonisation in Europe among asphalt mixture producers and highway agencies. The preferred test is currently the two-point bending test performed on trapezoidal specimens, which forms part of the French asphalt mixture design procedure.[2] However, other tests such as the four-point bending test on prismatic-shaped specimens and the indirect tensile test (ITT) on cylindrical-shaped specimens are still being used throughout Europe.

One example of the indirect tensile configuration is the indirect tensile fatigue test (ITFT) that forms part of the suite of tests undertaken with the Nottingham Asphalt Tester (NAT).[3] This simple and inexpensive test method has the advantage of being able to utilise cylindrical specimens manufactured in the laboratory or cored from a pavement. However, the ITFT, like other ITT arrangements, suffers from concerns over the absence of stress reversal, the accumulation of permanent deformation and the potential under high loads and/or high temperatures for either compressive or shear failure to occur in the specimen. These concerns have been partly addressed by Read and Collop,[4] who found that under the recommended test conditions (120 ms loading time and test temperatures less than 30 °C) tensile failure is the dominant mode in asphalt mixture specimens.

This paper describes an assessment of the comparison between the ITFT, currently used as a routine practical method for evaluating the life to crack initiation of bituminous paving mixtures, and the preferred European two-point bending fatigue test. The two tests were used to determine the fatigue response of a standard UK asphalt mixture at two different test temperatures. In addition, an alternative fatigue failure definition to the traditionally used failure point was presented for both the two-point bending test and the ITFT.

2. EXPERIMENTAL PROGRAMME

2.1. Materials

The experimental investigation was carried out on a continuously graded 20 mm dense bitumen macadam (DBM)

Sieve size: mm	Specification limits: %		Midpoint: %	Design: %
	Minimum	Maximum		
28	100	100	100	100
20	95	100	97·5	97·3
14	65	85	75	75·7
10	52	72	62	60·8
6·3	39	55	47	49·3
3·35	32	46	39	39·6
0·3	7	21	14	12·9
0·075	2	9	5·5	8·1

Table 1. Aggregate gradation for 20 DBM mixture

asphalt mixture with a maximum aggregate size of 20 mm, in accordance with the specification for 20 mm size dense binder course mixtures in BS 4987-1: 2001.[5] An unmodified 40/60 penetration grade bitumen conforming to BS EN 12591: 2000[6] was used at a design binder content by mass of total mixture of 4·7%. The aggregate used to produce the asphalt mixture was a UK limestone, primarily composed of calcium carbonate, but also containing varying amounts of magnesium carbonate and siliceous mineral deposits. The particle size distribution of the 20 mm DBM mixture and the specification limits are given in Table 1 and illustrated in Fig. 1.

2.2. Test procedures

Two fatigue test methods were utilised in the experimental programme; the ITFT and the two-point bending cantilever test. In addition, indirect tensile stiffness modulus (ITSM) tests were performed in order to determine the stiffness modulus of the ITFT cylindrical specimens prior to fatigue testing. The stiffness modulus was used to calculate the initial horizontal strain in the ITFT.

2.3. Indirect tensile stiffness test

The well known ITSM test, defined in BS 213: 1993[7] and in BS EN 12697-26: 2004,[8] was used to determine the stiffness modulus of the cylindrical specimens prior to their fatigue testing in the ITFT. During the test a compressive load pulse is applied by means of a load actuator along the vertical diameter of a cylindrical specimen. The resultant (indirect tensile) peak transient deformation is measured along the horizontal diameter using linear variable displacement transducers (LVDTs), whereas the vertical load is measured using a load cell (Fig. 2).

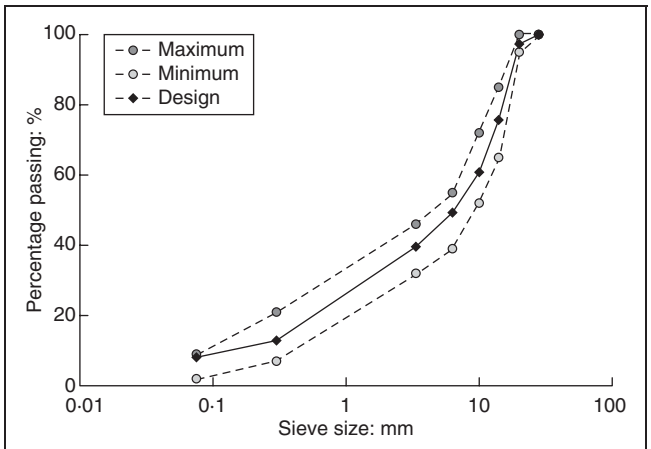

Fig. 1. Gradation curve for the 20 mm DBM

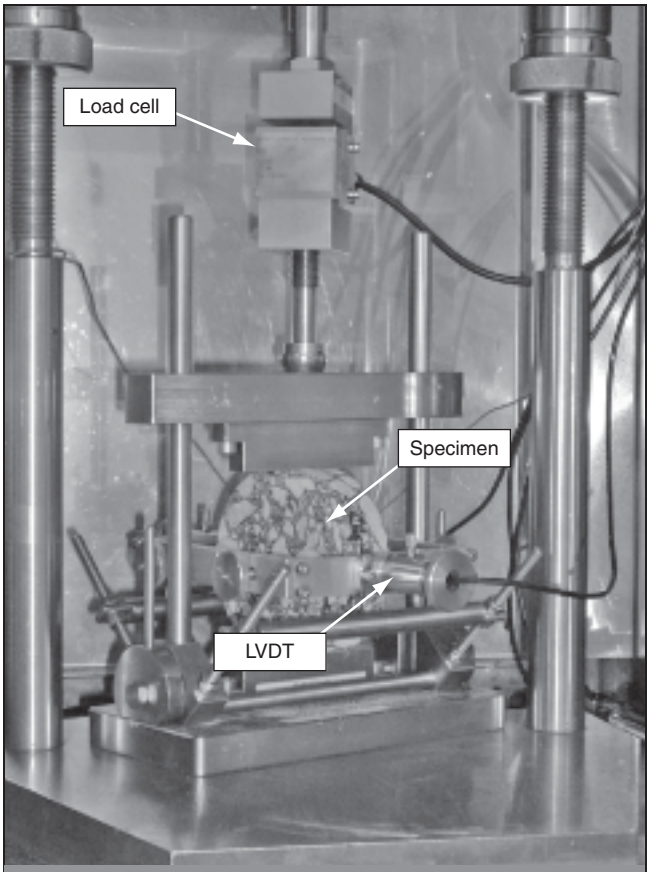

Fig. 2. Indirect tensile stiffness modulus test

In this work, the ITSM test was performed in accordance with the British Standard 213[7] using the following test parameters

(*a*) test temperature: 10 and 30 °C
(*b*) Poisson's ratio: 0·25 at 10 °C and 0·45 at 30 °C
(*c*) loading rise-time: 124 ms
(*d*) peak transient horizontal deformation: 5 μm.

The captured signals from the transducers were used to calculate the stiffness modulus as a function of vertical load, horizontal deformation, specimen dimensions and an assumed Poisson's ratio for the material. The relationship used to calculate stiffness modulus S_m (in MPa) is as follows[7]

$$S_m = \frac{L}{D \cdot t} \cdot (\nu + 0{\cdot}27) \quad (1)$$

where L is the peak value of the applied vertical load (N); D is the peak horizontal diametral deformation resulting from the applied load (mm); t is the mean thickness of the test specimen (mm); and ν is Poisson's ratio for the bituminous mixture at the test temperature.

During the ITSM test, five conditioning pulses are followed by five test pulses, which are used to determine an average stiffness modulus. The test is then repeated after rotating the

specimen through 90° and the average stiffness from the two tests is recorded as the stiffness modulus of the asphalt mixture specimen.

2.4. Indirect tensile fatigue test

The ITFT characterises the fatigue behaviour of bituminous mixtures under controlled load test conditions. The experimental arrangement of the ITFT is similar to that used for the ITSM but with slight modifications to the crosshead. In the ITFT (Fig. 3), displacement transducers are used to measure the vertical deformation instead of the deformation across the horizontal diameter of the specimen, as in the ITSM test. A cylindrical test specimen is subject to repeated compressive loading across the vertical diametrical plane. The resulting horizontal tensile stress $\sigma_{x,max}$ at the centre of the specimen in (kPa) is calculated as follows

$$\sigma_{x,max} = \frac{2 \cdot P_L}{\pi \cdot d \cdot t} \quad (2)$$

where P_L is the vertically applied line loading (kN); d is the diameter of the test specimen (m); and t is the thickness of the test specimen (m).

The resulting horizontal strain $\varepsilon_{x,max}$ [in (μstrain)] at the centre of the specimen can then be calculated using an assumed Poisson's ratio as follows

$$\varepsilon_{x,max} = \frac{\sigma_{x,max} \cdot (1 + 3\nu)}{S_m} \cdot 1000 \quad (3)$$

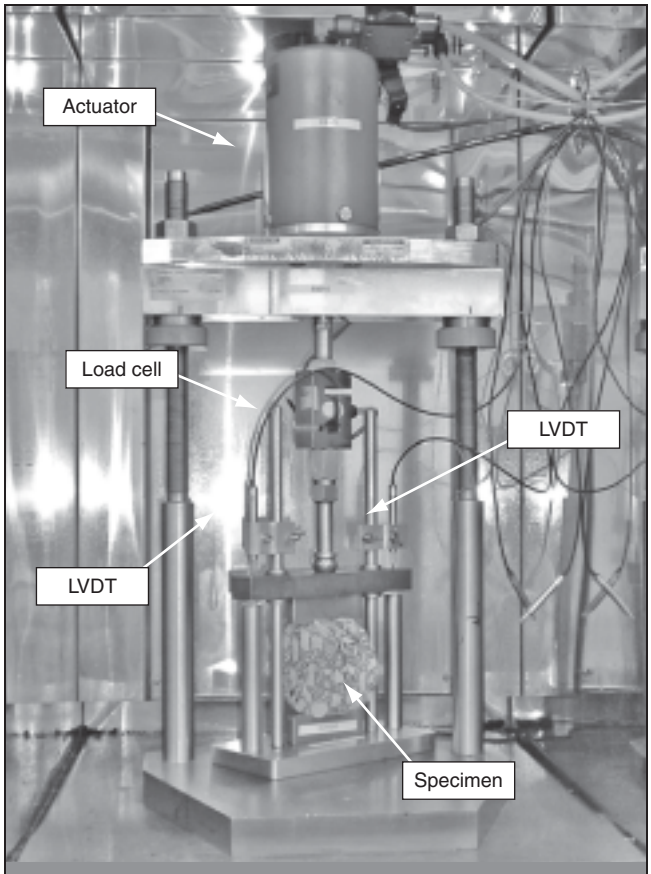

Fig. 3. Indirect tensile fatigue test

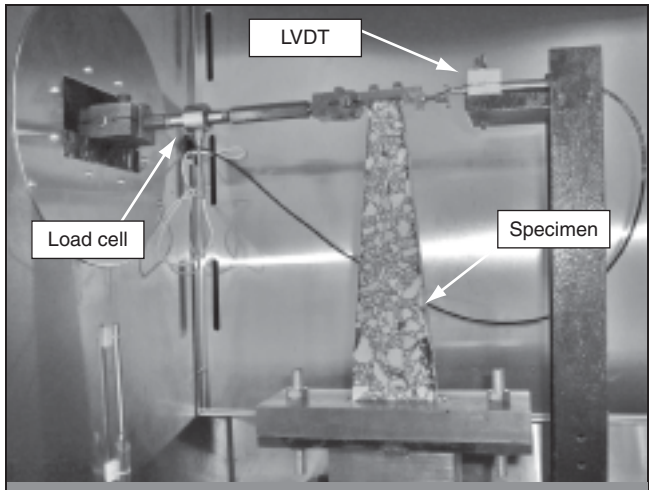

Fig. 4. Two-point bending test apparatus

where $\sigma_{x,max}$ is the maximum tensile stress at the centre of the specimen (kPa); ν is the assumed Poisson's ratio; and S_m is the indirect tensile stiffness modulus obtained from ITSM test performed on the same specimen (MPa).

The ITFT tests were performed using the following conditions

(*a*) test temperature: 10 and 30 °C
(*b*) Poisson's ratio: 0·25 at 10 °C and 0·45 at 30 °C
(*c*) loading condition: controlled-stress
(*d*) loading rise-time: 120 ms
(*e*) failure indication: 9 mm vertical deformation.

In terms of the failure criterion, the fracture life of the bituminous mixture was determined as the total number of load applications before fracture of the specimen occurred or a vertical deformation of 9 mm was achieved.

2.5. Two-point bending cantilever test

The two-point bending cantilever beam fatigue test was performed using an electro-magnetic actuator. This test can be carried out in two control modes; 'controlled strain (displacement)' and 'controlled stress (load)'. For this project, all the tests were carried out under controlled stress conditions since this is the mode of control used for the ITFT.

Under loading, the trapezoidal specimen is subjected to a sinusoidal zero-mean bending stress at a constant frequency. The applied load is measured by a load cell situated between the specimen and the actuator at the end (top) of the cantilevered specimen, while the deflection at the end of the specimen is measured by a displacement transducer (Fig. 4).

The trapezoidal specimens used in this study had a top width (*b*) of 25 mm, base width (*B*) of 70 mm with a constant thickness (*e*) of 25 mm and height (h) of 250 mm according to the European Standard EN 12697-24: 2004[9] that establishes the dimensions of the specimens by the maximum aggregate size of the bituminous mixture as shown in Fig. 5 and Table 2.

Analysis of the trapezoidal cantilever beam was carried out using conventional bending theory[10] resulting in the following

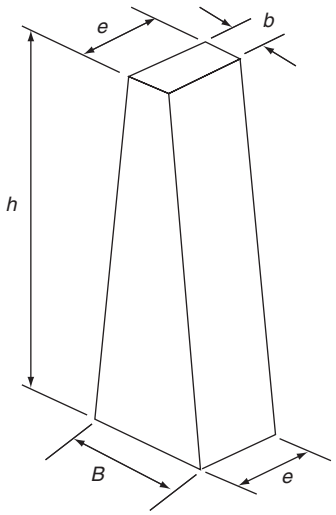

Fig. 5. Geometry of two-point bending trapezoidal specimens: EN 12697-24: 2004[9]

expression for the stiffness modulus E (in MPa) of the asphalt mixture

$$E = \frac{w \cdot l}{\delta_0 \cdot d \cdot b} \cdot \left[K_1 \cdot \frac{l^2}{d^2} + K_2(1 + \nu) \right] \quad (4)$$

where w is the horizontally applied load (kN); l is the length of the specimen (m); δ_0 is the deflection at top of beam (due to both bending and shear stresses) (mm); d is the top width (m); b is the thickness of the specimen (m); ν is assumed Poisson's ratio; and K_1, K_2 are coefficients depending on the geometry of the specimen (for this research it was found that $K_1 = 0{\cdot}37064$ and $K_2 = 1{\cdot}14402$).

The maximum value of tensile stress σ_{max} (in kPa) generated in the specimen is given by the following equation

$$\sigma_{max} = \sigma\left(x_{max} = \frac{l}{j-1}\right) = \frac{3}{2} \cdot \frac{l \cdot w}{b \cdot d^2 \cdot (j-1)} \quad (5)$$

where x_{max} is the distance from the point of loading of the section where the maximum value of tensile stress is achieved; j is the ratio between base and top width (specimen geometry chosen according to the European Specification[9] gives $j = 2{\cdot}8$).

Dimensions of the specimens	Type of mixture		
	$D \leq 14$ mm	$14 < D \leq 20$ mm	$20 < D \leq 40$ mm
B	56 ± 1 mm	70 ± 1 mm	70 ± 1 mm
b	25 ± 1 mm	25 ± 1 mm	25 ± 1 mm
e	25 ± 1 mm	25 ± 1 mm	50 ± 1 mm
h	250 ± 1 mm	250 ± 1 mm	250 ± 1 mm

Table 2. Dimensions of the specimens: EN 12697-24: 2004[9]

The resulting maximum strain ε_{max} (in μstrain) is then calculated as follows

$$\varepsilon_{max} = \frac{\sigma_{max}}{E} \cdot 1000 \quad (6)$$

where σ_{max} is the maximum value of tensile stress achieved in specimen (kPa); and E is the stiffness modulus (MPa).

2.6. Testing programme

The testing programme consisted of two sets of fatigue tests. The first part of the programme involved the fatigue assessment of the 20 mm DBM asphalt mixture using the two-point bending fatigue apparatus. Trapezoidal specimens were tested under the following conditions

(*a*) mode of loading: controlled stress
(*b*) temperatures: 10 and 30 °C
(*c*) frequency: 10 Hz.

The aim of the second part of the testing programme was to characterise the ITFT fatigue behaviour of the 20 mm DBM and compare these results with those obtained from the two-point bending tests. This was achieved by performing sets of indirect tensile tests under the following test conditions

(*a*) mode of loading: controlled stress
(*b*) temperatures: 10 and 30 °C
(*c*) frequency: 40 pulses per min.

Each ITFT cylindrical specimen was previously tested in the ITSM test in order to evaluate the stiffness modulus at the test temperature and Poisson's ratio. The specimens were then tested at different stress levels (100 to 2500 kPa) to give a spread of lives of approximately three orders of magnitude. Finally, comparisons have been made between the fatigue results obtained from the two different tests, conducted on the same material at two temperatures.

3. SPECIMEN COMPACTION AND PRODUCTION

An essential part of any asphalt mixture mechanical property investigation is to ensure that the specimens are suitably compacted using a laboratory compaction method that is able to produce uniform specimens that closely represent field compacted mixtures.

3.1. Specimen geometry

Once the materials (bitumen, aggregate and filler) had been uniformly mixed according to EN 12697-35: 2002,[11] the calculated amount of hot mixture was poured into pre-heated square moulds (305 × 305 mm) and compacted to the required slab thickness using the Nottingham Roller Compactor according to EN 12697-33: 2003.[12] This compaction method was chosen since it reproduces in situ characteristics. The ITFT and two-point bending test samples were obtained from these slabs whose target air voids content was fixed at 4%.

The fatigue investigation was conducted on two different types of specimens: cylindrical specimens (100 mm diameter with a height of 40 mm) for the ITFT and trapezoidal specimens (dimensions for $14 < D \leq 20$ mm mixture in Table 2) for the cantilever two-point beam fatigue test. Samples were cored or cut from the slabs manufactured in the 305 mm square moulds

with the depth (height) of the slabs dependent on the type of test samples to be extracted.

3.2. Sawing and trimming

Following compaction, the slabs of asphalt mixture were allowed to cool to room temperature, stripped from the moulds and cored or sawed to produce specimens for testing as detailed below.

3.3. Cylindrical specimens

To obtain specimens for the ITFT, several 80 mm high slabs were produced and five cores (100 mm in diameter) were taken from each slab. Cylindrical specimens, 100 mm in diameter and 40 mm high, were then obtained by trimming the top and the bottom of each core using a masonry saw in order to eliminate those parts that usually contain higher air voids content or imperfections.

3.4. Trapezoidal specimens

Trapezoidal fatigue test specimens were manufactured from 90 mm high slabs using a masonry saw and a purpose-built clamping device (Fig. 6). Four different sawing procedures were followed in order to evaluate the best method to rapidly obtain a large number of specimens from the same slab but still guarantee an acceptable level of homogeneity in terms of air void distribution.

Two of the procedures consisted of sawing the specimens along horizontal planes in the direction of compaction and in a normal direction with respect to compaction. Using these procedures it was possible to produce 10 specimens per slab. The other two procedures consisted of sawing the slabs along vertical planes, in the direction of compaction and in the orthogonal direction respectively. In these cases nine specimens per slab were obtained.

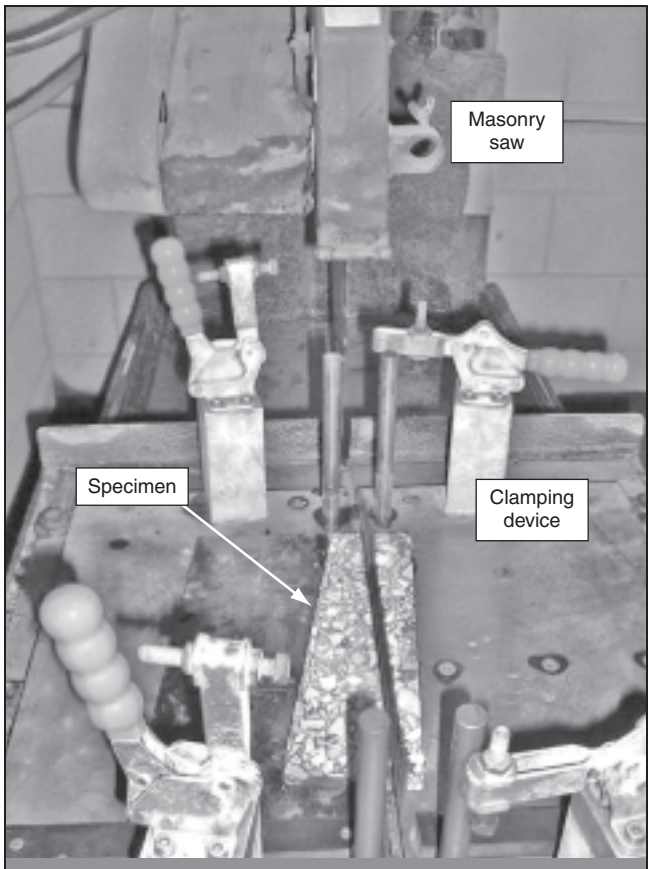

Fig. 6. Jig for sawing trapezoidal specimens from compacted asphalt mixture slabs

3.5. Air void distribution

After the specimens were trimmed, they were placed on absorbent paper and allowed to dry at room temperature. The dimensions of each specimen were measured and the bulk densities of the specimens were determined as detailed in BS EN 12697-6: 2002[13] using self-adhesive foil tape as sealant. The bulk densities were used together with the maximum theoretical density, determined on loose mixture samples by the volumetric procedure BS EN 12697-5: 2002,[14] to calculate the percentage of air voids of each test specimen.

A study on density and air void content was carried out on the trapezoidal specimens to determine the homogeneity of samples to be used in the two-point bending fatigue test. Each specimen was cut into five subsections (50 mm high) and the density and air void content determined. A degree of non-homogeneity was observed due to several reasons including boundary effects, non-homogeneous compaction and the relatively small size of the trapezoidal specimens compared to the 20 mm maximum aggregate. However, in terms of the effect of sawing and trimming, all four procedures produced similar specimens in terms of volumetrics. As the variability of air voids affects the mechanical properties of test specimens and may even result in a shifting of the fracture zone in the trapezoidal specimens, specimens taken from the centre of the slab rather than the edges were used for testing. In addition, to remove any influence of compaction orientation on the fatigue results, only one sawing procedure was used in the study.

3.6. Specimen gluing and conditioning

Trapezoidal and cylindrical specimens that met the target air void content were marked and stored in a dry atmosphere on one of their flat faces at a temperature of 5 °C to prevent distortion according to DD 213: 1993[7] and BS EN 12697-26: 2004.[8] Specimens were only removed from this controlled environment to be bonded to test end plates (trapezoidal specimens only) and to be conditioned at test temperature (for at least 4 h prior to testing according to EN 12697-24: 2004[9]). Subsequently, they were tested in a constant temperature cabinet at the controlled test temperature.

The trapezoidal specimens were bonded to steel end plates using epoxy resin to enable them to be fitted to the cantilever test apparatus. The gluing of the end plates was undertaken according to the European specification EN 12697-24: 2004[9] with each trapezoidal specimen being glued by its large base in a groove 2 mm deep made on a steel base 20 mm thick. This operation was carried out on a special jig (Fig. 7) to ensure the correct specimen positioning on the base during the resin hardening process. The glue film was kept as thin as possible and the resin was allowed to harden for a minimum period of 24 h prior to testing.

4. TWO-POINT BENDING FATIGUE TEST

4.1. Fatigue failure analysis

The fatigue data generated from the two-point bending test were analysed by studying the evolution of complex (stiffness)

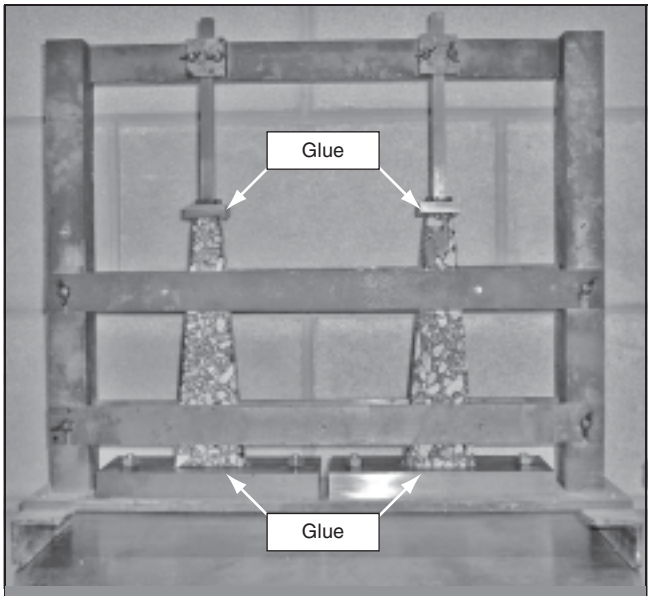

Fig. 7. Jig for gluing trapezoidal specimens to two-point bending apparatus end plates

modulus with the number of cycles as shown in Fig. 8. This curve shows the following three distinctive phases of response as reported in previous fatigue studies.[15,16]

(*a*) Phase I (adaptation phase). This phase is characterised by a rapid decrease in stiffness ratio (or stiffness) due to repetitive excitation of the test specimen. A precise explanation of this decrease is not clear but it has been suggested that it is possibly caused by the combined effects of fatigue damage, localised heating in the specimen and thixotropy. Although part of the initiation phase of fatigue, this adaptation phase is generally thought to be a testing artefact that is usually rapidly recoverable if the test is halted before micro-crack coalescence (propagation phase) begins.

(*b*) Phase II (quasi-stationary phase). This phase corresponds to the period where the role of fatigue on the stiffness decrease is dominant. During this phase, any artefact effects such as thermal heating and thixotropy can be considered to be small compared to the dominant effect of fatigue damage. Together with phase I they make up the fatigue initiation phase up to the point were micro-cracks begin to coalesce.

(*c*) Phase III (failure phase). This phase corresponds to the local crack propagation phase. Macro-cracks begin to develop and global failure is obtained at the end of this phase.

Although dividing the evolution of stiffness into the three phases is useful in terms of understanding the process of fatigue damage, determining the actual point of fatigue failure has been a controversial topic with various definitions involving phenomenological as well as energy approaches being proposed and used.[17–25] In this study the failure criterion used for the two-point bending fatigue test under controlled stress conditions was a reduction of the initial stiffness of 90% (10% retained stiffness), which can be considered to coincide with complete failure (fracture) of the test specimen. In addition, two further definitions of failure were considered consisting of a 50% reduction in initial stiffness (more commonly used with controlled strain fatigue tests) and a function involving the stiffness of the specimen and the number of load cycles. This stiffness procedure involved plotting the product of the ratio of asphalt mixture stiffness to initial stiffness and the number of cycles

$$nE^*/E^*_{\text{initial}} \quad (7)$$

where E^* is complex stiffness of the trapezoidal specimen; and n is the number of load cycles.

Fatigue failure was then considered to occur at the maximum value (peak) of the $nE^*/E^*_{\text{initial}}$ against n plot.[26] This representation of fatigue failure is considered a more accurate and reasonable means of defining fatigue failure than simply determining failure as an arbitrary condition such as a 50 or 90% reduction of initial stiffness. The basis of the $nE^*/E^*_{\text{initial}}$ against n plot as a means of defining the fatigue failure point is illustrated in Fig. 9 which shows changes in dynamic modulus and phase angle due to fatigue damage accumulation in bituminous materials.

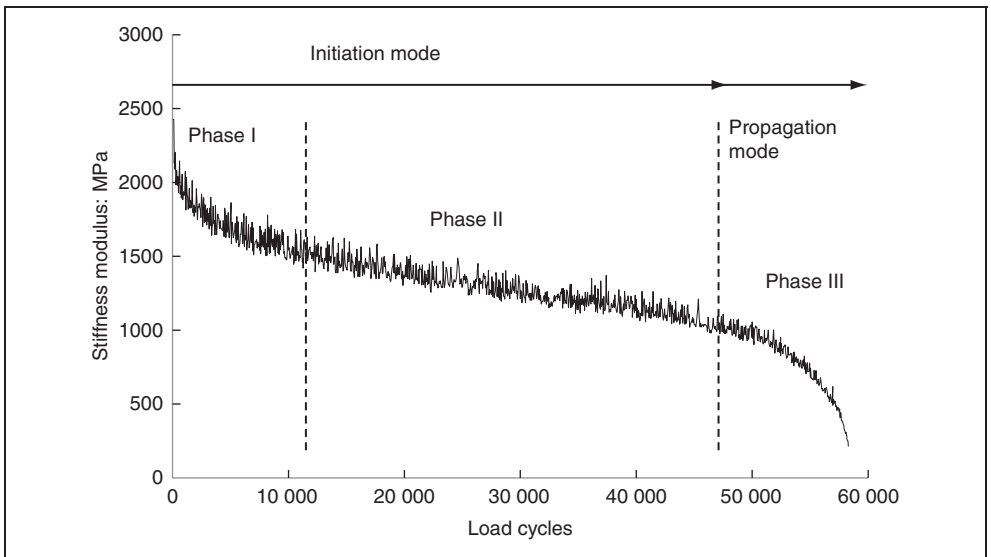

Fig. 8. Stiffness modulus versus load cycles evolution curve from the two-point bending test at 30 °C (specimen 04-1908)

As previously described and shown in Fig. 9, fatigue specimens experience rapid damage in the early stage of a test followed by a period where the rate of damage remains fairly constant representing controlled micro-cracking. This is followed by an accelerated period of damage indicating macro-cracking. In terms of the phase angle, there is an increase to a peak value followed by a sharp drop as loading continues. This peak in phase angle has been successfully used as an indication of the fatigue failure point by various researchers.[27,28] The gradual increase in phase angle is due

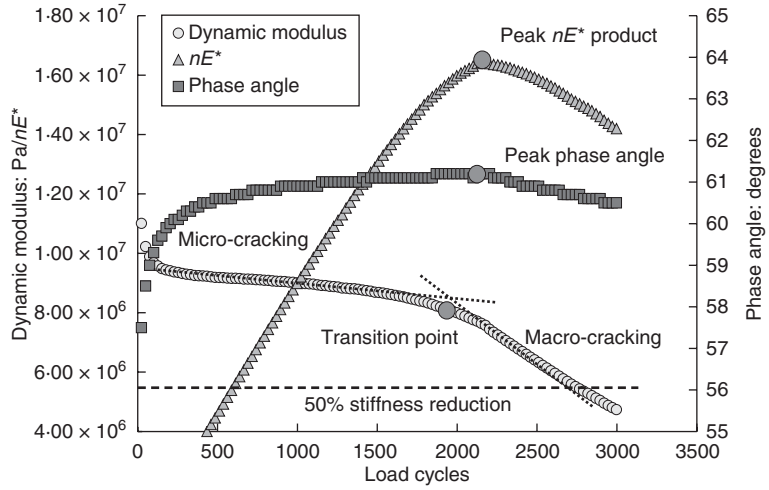

Fig. 9. Fatigue failure definition points for standard fatigue test

to an increased viscous response of the material as damage accumulates in the form of micro-cracks and the test specimen experiences a reduction of its elasticity. However, once the specimen experiences significant structural changes due to macro-cracking, it can no longer accumulate damage and consequently the phase angle decreases rapidly.[29]

In addition to the use of the peak phase angle as an indication of fatigue failure, a second point can be identified based on a more detailed assessment of the rate of change of stiffness with load cycles. Fig. 9 shows that there are two rates of change in dynamic modulus against load cycles representing micro-cracking and macro-cracking, respectively, and a transition point between these two rates. This transition point represents the shift from micro- to macro-cracking and has also been successfully used as an indicator of the fatigue failure point.[26,30] Kim *et al.*[30] also showed that there is a good match between these two fatigue failure points, which can also be seen in Fig. 9.

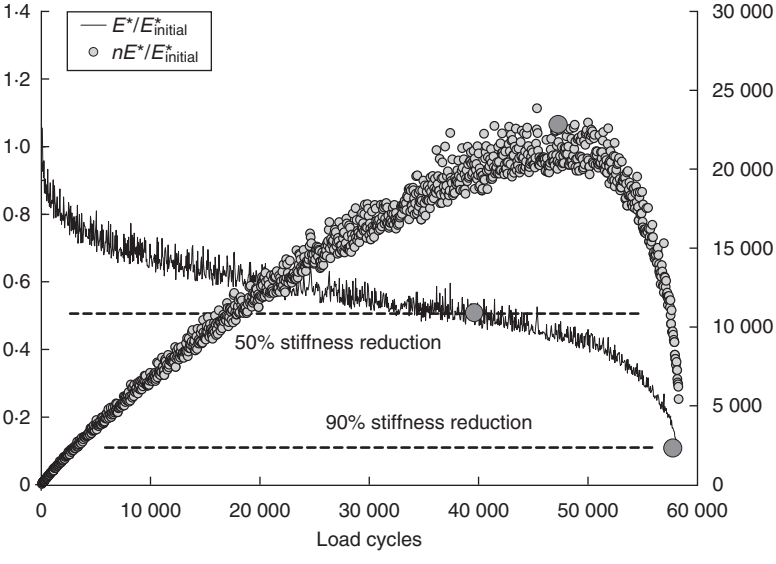

Fig. 10. Fatigue failure points for the two-point bending test at 30 °C (specimen 04-1908)

The third fatigue failure point associated with the peak of $nE^*/E^*_{\text{initial}}$ can also be seen to coincide with the peak phase angle and the stiffness rate transition point. In addition, this final definition has the advantage of not relying on an accurate measure of phase angle to determine fatigue failure life. Three fatigue lives were therefore produced for each fatigue test as shown in Figs 10 and 11 for a two-point bending test at 30 and 10 °C respectively.

Figure 10 shows that at 30 °C, the failure definitions produce three different fatigue lives for the same test with the peak $nE^*/E^*_{\text{initial}}$ value being between the shorter 50% stiffness reduction and longer 90% stiffness reduction fatigue lives. The results at 10 °C in Fig. 11 show a different trend with the fatigue lives at 50 and 90% stiffness reduction being very similar due to the rapid coalescence of micro-cracks and movement of the fatigue response from phase II to phase III for the stiffer asphalt material. In this case the peak $nE^*/E^*_{\text{initial}}$ failure definition provides a more conservative fatigue life.

The fatigue responses in Figs 10 and 11 show the two extremes in terms of stiffness evolution, comprising a consistent decrease in stiffness in phase II followed by a smooth transition into phase III for the test undertaken at 30 °C. This can be compared with the lower rate of stiffness decrease in phase II with a rapid and sharp decrease in stiffness in phase III at 10 °C. In addition, the rapid decrease in stiffness ratio in phase I is significantly more prominent at the higher temperature (Fig. 10) than at 10 °C in Fig. 11. The variability associated with the decrease in stiffness during phase II together with the uncertainty associated with selecting the initial stiffness of the test specimen has serious implications in terms of defining the fatigue life to failure when using arbitrary failure definitions such as the 50 and 90% reduction in initial stiffness. This is illustrated in Fig. 12 where, depending on how the initial stiffness is defined (position 1, 2 or 3), the fatigue life associated with the 50% stiffness reduction criterion can vary from approximately 35 000 to 55 000 cycles. In addition, the position of the fatigue failure point varies from within phase II, at the transition between phase II and III and finally in phase III.

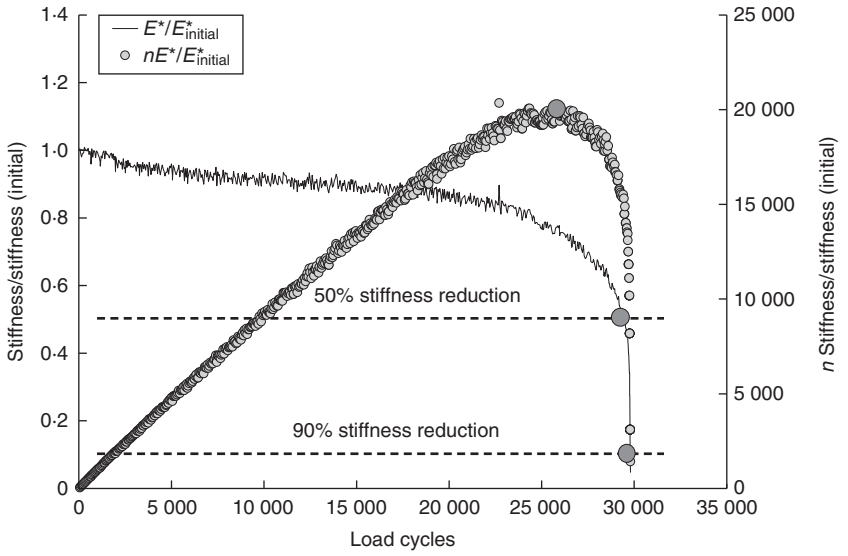

Fig. 11. Fatigue failure points for the two-point bending test at 10 °C (specimen 04-1954)

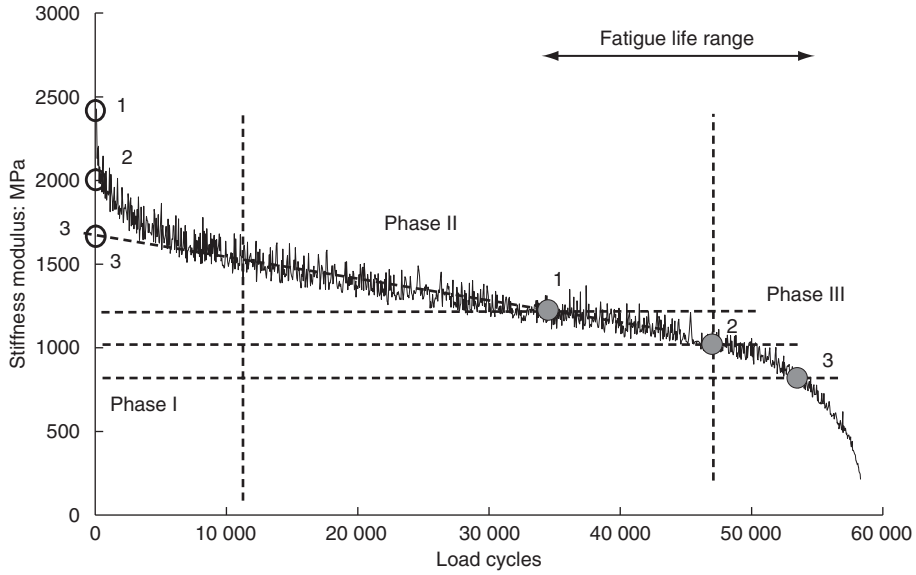

Fig. 12. Variability in fatigue life as defined by a 50% reduction in initial stiffness modulus

For this reason, the 50% reduction in initial stiffness failure definition was not used in calculating the fatigue relationships for the two-point bending tests.

4.2. Failure pattern

The position of maximum tensile stress in the trapezoidal fatigue tests can be found by differentiating the bending stress equation (equation (5)) and setting the derivative equal to zero. The maximum value of tensile stress along the standard specimen is therefore achieved at (Fig. 13):

$$x_{max} = \frac{5}{9} l \quad (8)$$

where l is the length of the specimen; and x_{max} is the distance from point of loading where $\sigma = \sigma_{max}$.

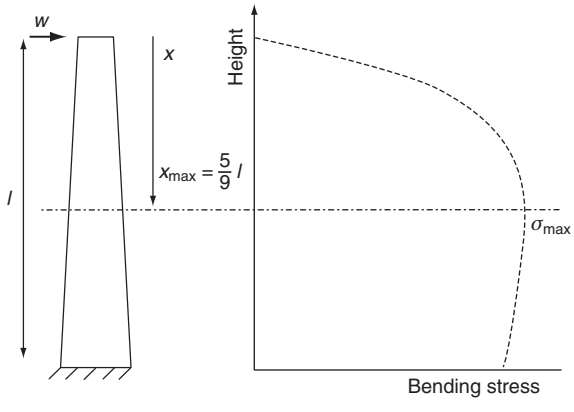

Fig. 13. Stress distribution in a two-point bending trapezoidal specimen

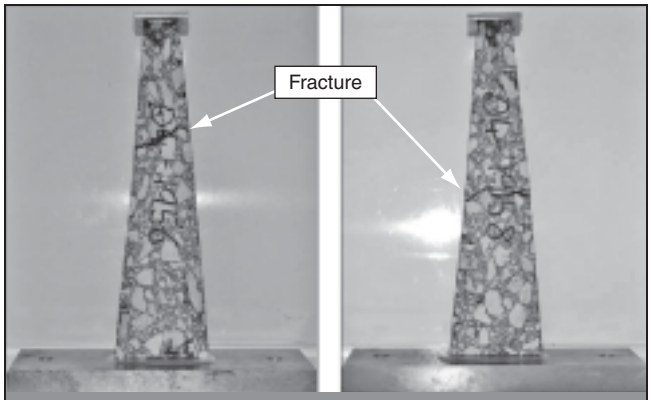

Fig. 14. Failure patterns for trapezoidal specimens subjected to two-point bending

Specimen ID	Strain: μstrain	N_f (10%)	N_f (50%)	N_f (nE^*/E^*_{ini})
04-1903	332	5674	2794	4450
04-1904	231	23 594	12 350	18 300
04-1905	803	1374	1154	1050
04-1907	215	6974	4950	5100
04-1908	170	58 294	41 050	47 500
04-1909	547	624	450	450
04-1910	652	594	335	475
04-1911	864	375	200	250

Table 3. Fatigue lives as a function of failure definition from two-point bending fatigue test at 30 °C

Specimen ID	Strain: μstrain	N_f (10%)	N_f (50%)	N_f (nE^*/E^*_{ini})
04-1954	136	29 794	29 500	25 950
04-1956	110	57 954	57 600	53 450
04-1957	150	37 214	36 750	34 550
04-1958	85	422 874	418 800	388 200
04-1959	182	7414	7200	6400
04-1961	156	11 774	11 550	10 450
04-1963	72	339 474	334 250	305 250

Table 4. Fatigue lives as a function of failure definition from two-point bending fatigue test at 10 °C

In general, the fatigue failures, as shown in Fig. 14, occurred within the middle third of the trapezoidal specimen and therefore in close proximity to the region of maximum tensile stress.

4.3. Fatigue relationships

The fatigue lives based on the three fatigue failure definitions are presented in Tables 3 and 4. The classical Wöhler curves[31] of strain/stress against fatigue life were used to represent the fatigue data generated from the two-point bending tests

$$N_f = a\varepsilon_0^{-b} \quad (9)$$

where: N_f is the fatigue life; ε_0 is the initial tensile strain (microstrain) or σ_0 (initial tensile stress); and a, b are experimentally determined coefficients.

The fatigue results, based on the maximum tensile stress plotted against the number of cycles to failure are shown in Fig. 15. The results show different fatigue lines for the two temperatures and failure definition points (90% stiffness reduction and peak $nE^*/E^*_{initial}$ against n). Although the fatigue functions are almost identical at 10 °C, there is a slight shifting of the peak $nE^*/E^*_{initial}$ against n fatigue curve at 30 °C from that obtained based on the 90% stiffness reduction failure point. The results were also plotted in terms of tensile strain,[32] using the peak $nE^*/E^*_{initial}$ failure point, in Fig. 16. A unique fatigue function was determined for each temperature although the data could have been used to form a single fatigue relationship regardless of test temperature with an R^2 value of 0·90.

5. INDIRECT TENSILE FATIGUE TEST

5.1. Fatigue failure analysis

The ITFT failure point is defined as 9 mm of permanent vertical deformation.[4] The evolution of vertical deformation against loading cycles for an ITFT test at 30 °C can be seen in Fig. 17. The shape of the curve is inverted compared to the stiffness evolution against loading cycles curve from the two-point bending test. It is therefore possible to produce a normalised

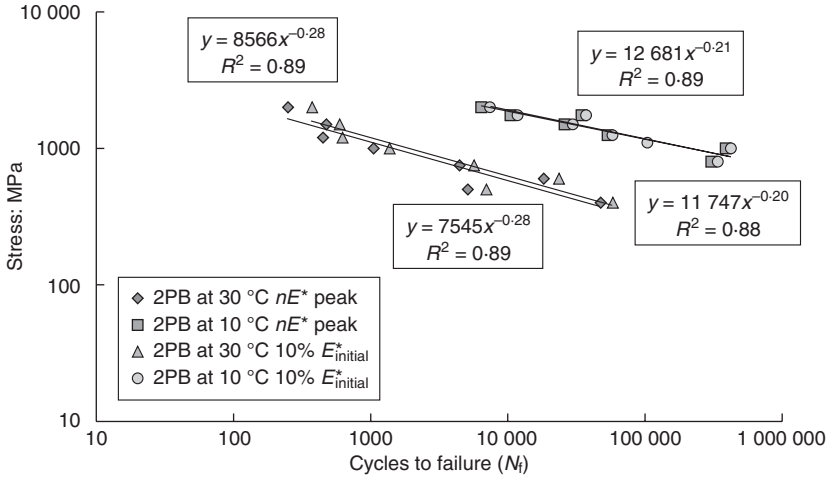

Fig. 15. Fatigue life as a function of applied stress level for two-point bending fatigue tests

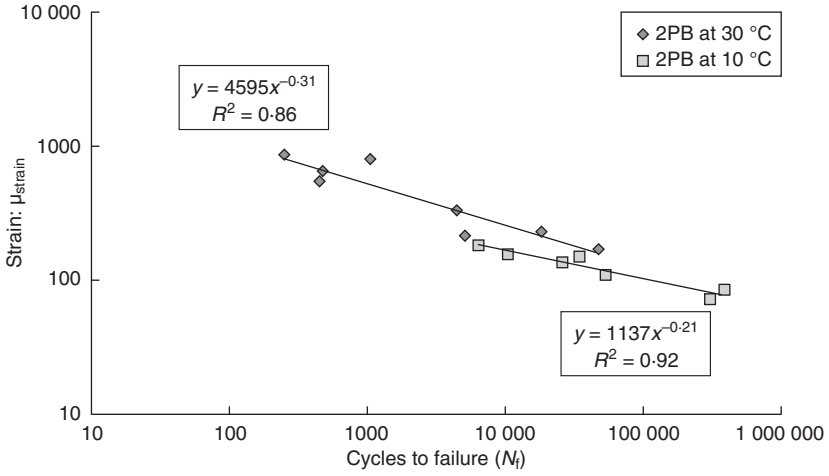

Fig. 16. Standard strain-based fatigue relationships for two-point bending fatigue tests at 10 and 30 °C

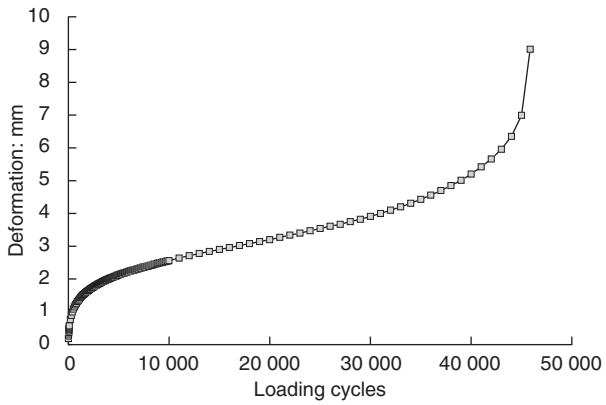

Fig. 17. Vertical deformation versus loading cycles for ITFT test at 30 °C (specimen 04-1532C)

creep stiffness ($E_{creep}/E_{creep\ initial}$) versus loading cycles (n) curve similar to the curves in Figs 10 and 11 as shown in Fig. 18. Although fundamentally this plot cannot be considered to represent fatigue damage, it is still an indication of overall material damage and therefore can be used to define the fatigue failure points for ITFT specimens rather than simply using the arbitrary 9 mm vertical deformation point. The three failure points for specimen 04-1532C at 30 °C are shown in Fig. 18. In a similar manner to the two-point bending test, three fatigue lives were therefore determined for each of the ITFT test specimens at both 10 and 30 °C.

5.2. Failure pattern

As mentioned previously, the indirect tensile ITFT is often accompanied by a combination of fatigue mechanisms and permanent deformation with larger amounts of permanent deformation occurring at higher temperatures.[24] Fig. 19 shows two different types of failure observed during testing. In general, fatigue tests carried out at 10 °C resulted in complete splitting of the specimens along the vertical plane, whereas specimens tested at 30 °C deformed plastically until the limiting vertical deformation of 9 mm was achieved. In this case localised deformations were also observed at the edge of the loading strips. What effect this difference in failure pattern has on fatigue life is assessed in the following sections.

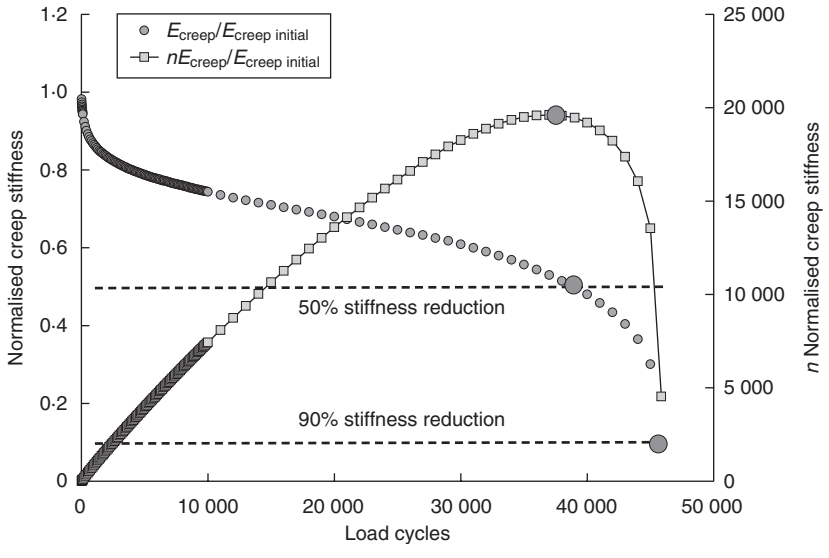

Fig. 18. Fatigue failure points for the indirect tensile test at 30 °C (specimen 04-1532C)

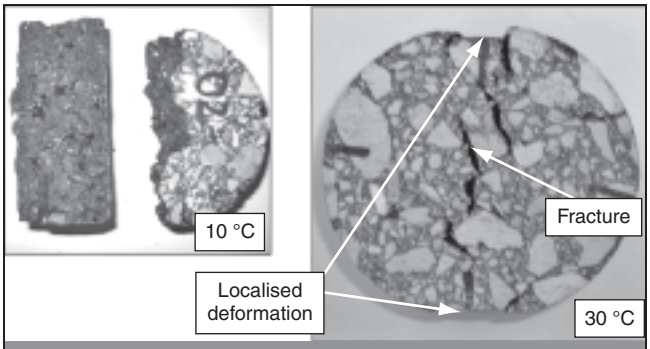

Fig. 19. Indirect tensile fatigue test failure patterns at 10 and 30 °C

5.3. Fatigue relationships

The stiffness values for the ITFT specimens as determined using the ITSM test are presented in Tables 5 and 6. The dimensions and air void content of the specimens are also included.

The initial strain level (computed using the stiffness values in Tables 5 and 6 and equation (3)) together with the three fatigue lives as a function of failure point definition method are presented in Tables 7 and 8. The results are also plotted in terms of tensile strain in Fig. 20, with the fatigue lives being based on the peak '$nE_{creep}/E_{creep\ initial}$' failure definition. As with the two-point bending test, a unique fatigue function was determined for each temperature, although once again the data could have been used to form a single fatigue relationship regardless of test temperature with an R^2 value of 0·95.

6. COMPARISON OF TEST METHODS

Studies comparing the fatigue results from various fatigue testing methods have tended to produce conflicting conclusions with regard to the relationship between ITT and two-point bending[4,16] Di Benedetto *et al.*[16] found that the ITT method produced shorter fatigue lives when compared with bending

Specimen ID	Diameter: mm	Height: mm	Air voids: %	Stiffness: MPa		
				0 °	90 °	Average
04-1531C	98	40	2·7	1421	1396	1409
04-1531D	98	43	3·3	1381	1496	1439
04-1531E	98	40	2·6	1563	1591	1577
04-1532A	98	41	4·1	1437	1307	1372
04-1532B	98	40	3·0	1340	1305	1323
04-1532C	98	40	2·3	1743	1733	1738
04-1532D	98	41	2·8	1566	1424	1495
04-1532E	98	40	3·2	1360	1471	1416

Table 5. Stiffness modulus results from the ITSM at 30 °C

Specimen ID	Diameter: mm	Height: mm	Air voids: %	Stiffness: MPa		
				0 °	90 °	Average
04-1529B	98	40	2·8	9935	8990	9463
04-1529E	98	40	2·9	9005	8807	8906
04-1530A	98	41	3·0	8998	8356	8677
04-1530B	98	41	3·5	8341	7620	7981
04-1530C	98	40	2·6	7799	7153	7476
04-1530E	98	42	3·1	7829	7448	7639
04-1531A	98	41	2·7	8244	7545	7895
04-1531B	98	41	3·1	8586	8362	8474

Table 6. Stiffness modulus results from the ITSM at 10 °C

Specimen ID	Strain: μstrain	N_f (10%)	N_f (50%)	N_f ($nE_{creep}/E_{creep\ initial}$)
04-1531C	1001	65	54	50
04-1531D	163	6394	4800	4500
04-1531E	343	1069	650	750
04-1532A	1028	35	30	30
04-1532B	1493	32	30	25
04-1532C	68	45 863	39 000	37 000
04-1532D	534	149	105	100
04-1532E	232	2342	1450	1700

Table 7. Fatigue lives as a function of failure definition from ITFT at 30 °C

Specimen ID	Strain: μstrain	N_f (10%)	N_f (50%)	N_f ($nE_{creep}/E_{creep\ initial}$)
04-1529B	111	36 715	35 000	31 500
04-1529E	196	8523	8500	7900
04-1530A	303	1800	1800	1700
04-1530C	94	161 876	157 500	145 000
04-1530E	252	6100	6100	5700
04-1531A	89	127 516	110 000	110 000
04-1531B	103	36 529	33 000	31 000

Table 8. Fatigue lives as a function of failure definition from ITFT at 10 °C

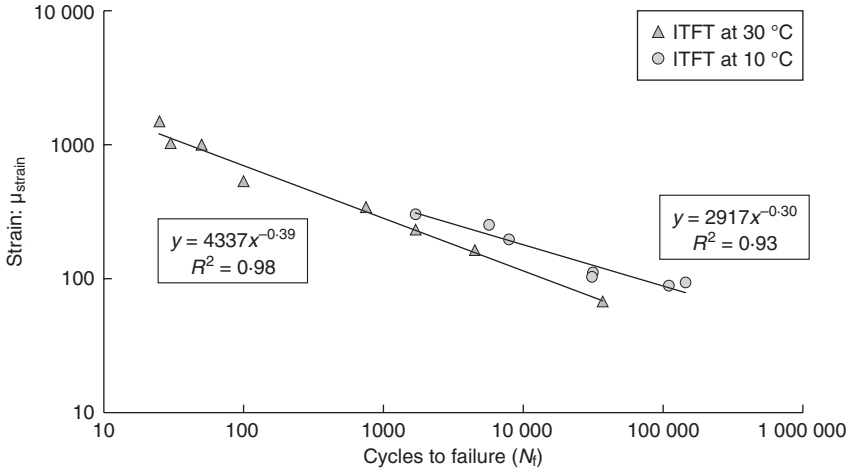

Fig. 20. Standard strain-based fatigue relationships for indirect tensile fatigue tests at 10 and 30 °C

tests including two-point bending. However, the ITT used in their study had continuous sinusoidal loading compared to the pulsed loading with significant rest periods used with the ITFT. In contrast, Read and Collop[4] found good agreement between the ITFT, two-point trapezoidal cantilever and uniaxial tension–compression test configurations for a range of asphalt mixture types. They attributed the good correlation between ITFT and two-point bending to the extended fatigue life associated with the rest periods used with the ITFT loading but warned that this good agreement may only be valid for the specific test conditions used in their research.

Prior to considering the fatigue relationship between the ITFT and two-point bending test, the average air voids content and stiffness modulus for the four combinations of test method and test temperature were compared in Table 9. On average the trapezoidal specimens tended to have a lower air void content compared with the cylindrical specimens. This, together with the shorter equivalent loading time, meant that the stiffness values for the two-point bending tests were higher than those found for the ITT configuration.

Fatigue test	Air voids: %		Stiffness: MPa	
	Average	CoV: %	Average	CoV: %
2PB at 30 °C and 10 Hz	2·6	16	2198	18
ITFT at 30 °C and 120 ms	3·0	18	1470	9
2PB and 10 °C and 10 Hz	2·8	30	11 297	3
ITFT at 10 °C and 120 msec	3·0	10	8313	8

Table 9. Comparison of air voids and stiffness modulus for two-point bending and ITFT tests

The fatigue functions at 10 and 30 °C for the ITFT and two-point bending fatigue tests were combined to form one function for each fatigue test in Fig. 21. The 90% initial stiffness (relative condition for ITFT) reduction failure point was used with the fatigue functions having an R^2 value of 0·90 for the two-point bending and 0·95 for the ITFT. The functions in Fig. 21 confirm previous research[16,24] with the fatigue life for the 20 mm DBM asphalt mixture being shorter for the indirect tensile

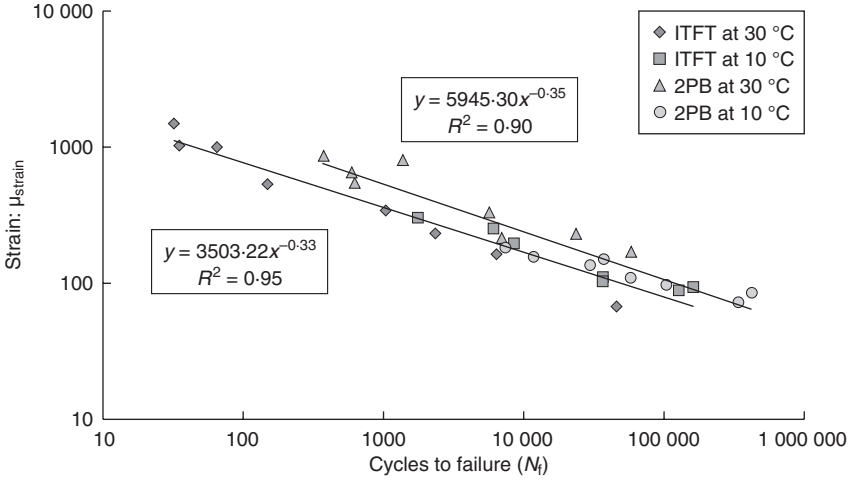

Fig. 21. Standard strain-based fatigue relationships for indirect tensile and two-point bending fatigue tests at 10 and 30 °C based on a 90% decrease in initial stiffness failure point

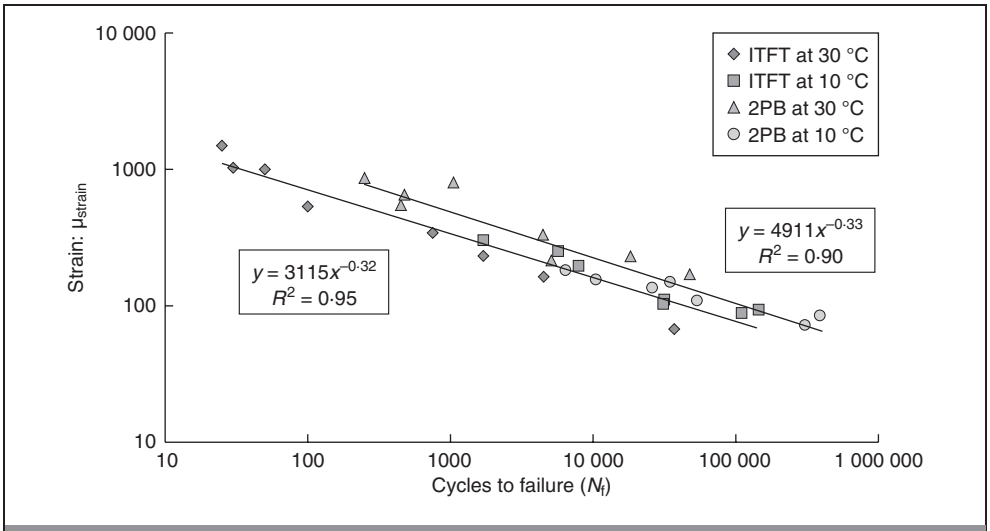

Fig. 22. Standard strain-based fatigue relationships for indirect tensile and two-point bending fatigue tests at 10 and 30 °C based on the peak $nE^*/E^*_{initial}$ ($nE_{creep}/E_{creep\ initial}$) failure point

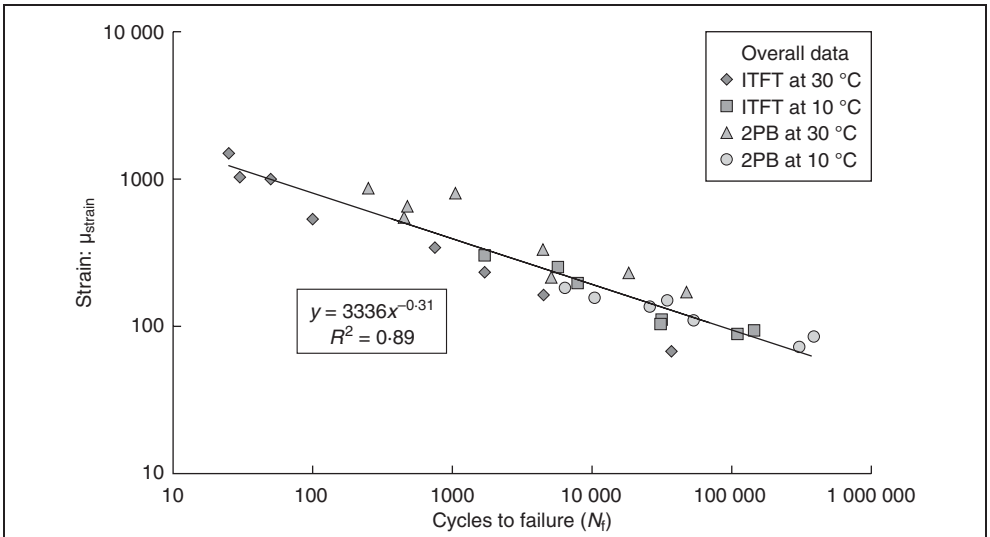

Fig. 23. Combined single fatigue relationships for fatigue tests at 10 and 30 °C based on the peak $nE^*/E^*_{initial}$ and $nE_{creep}/E_{creep\ initial}$ failure point

configuration compared to the two-point bending. The effect of failure point on the comparison of the two tests was investigated by plotting the fatigue results determined using the peak $nE^*/E^*_{initial}$ and $nE_{creep}/E_{creep\ initial}$ failure points instead of the 90% stiffness reduction. The results for the ITFT and two-point bending test are shown in Fig. 22. The results show a similar trend to that seen in Fig. 21, although the difference can now be quantified as a simply horizontal shifting of the fatigue lines as their slopes are identical.

Although the results shown in Figs 21 and 22 appear to contradict the conclusions based on the study undertaken by Read and Collop,[4] it is possible to combine the fatigue results from the two tests to form one fatigue function as shown in Fig. 23. The R^2 value for this unique fatigue function is 0·89 and is identical to the R^2 value obtained for a 20 mm DBM asphalt mixture tested by Read and Collop.[4]

7. CONCLUSIONS

The findings from the fatigue test investigation showed that fatigue results are sensitive to testing conditions (temperatures and loading times) as well as testing methods. Separate fatigue functions were produced for the four test method and temperature combinations based on an initial tensile strain against fatigue life relationship. The ITFT produced shorter fatigue lives for the 20 mm DBM asphalt mixture compared to the two-point bending fatigue test. However, although the ITT configuration ITFT produced shorter fatigue lives, it was possible to combine all four separate fatigue functions to produce one unique function for the 20 mm DBM asphalt mixture at a relatively high R^2 value.

In addition to the tradition 90% reduction in initial stiffness fatigue failure point, an alternative failure definition was also incorporated in the study. This failure point was based on the transition between the quasi-stationary phase associated with a uniform stiffness decrease and the development of micro-cracks and failure phase associated with localised crack propagation. The transition point (fatigue failure point) was determined by taking the peak of $nE^*/E^*_{initial}$ (or $nE_{creep}/E_{creep\ initial}$ for the ITSM) against loading cycles. This fatigue failure definition was then used to compare the merits of the indirect tensile ITFT against the two-point bending test.

In general the peak of $nE^*/E^*_{initial}$ (or $nE_{creep}/E_{creep\ initial}$ for the ITSM) against loading cycles failure definition was found to predict a slightly more conservative fatigue life compared to the traditional 90% reduction in initial stiffness.

REFERENCES

1. Di Benedetto H., Francken L. and De La Roche C. Fatigue of bituminous mixtures: different approaches and RILEM interlaboratory tests. *Proceedings of the Fifth International RILEM Symposium*, Lyon, France. Balkema, Rotterdam, The Netherlands, 1997, pp. 15–26.
2. Corte J.-F. and Serfass J.-P. The French approach to asphalt mixture design: a performance-related system of specifications. *Journal of the Association of Asphalt Paving Technologists*, 2000, **69**, 794–834.

3. Cooper K. E. and Brown S. F. Developments of a simple apparatus for the measurement of the mechanical properties of asphalt mixes. *Proceedings of the Eurobitume Symposium*, Madrid. Eurobitume, Brussels, Belgium, 1989, pp. 494–498.
4. Read J. M. and Collop A. C. Practical fatigue characterisation of bituminous paving mixtures. *Journal of the Association of Asphalt Paving Technologists*, 1997, **66**, 74–108.
5. British Standards Institution. *Coated Macadam (asphalt concrete) for Roads and other Paved Areas. BS 4987: Part 1 Specification for Constituent Materials and for Mixtures*. British Standards Institution, London, 2001.
6. British Standards Institution. *Bitumen and Bituminous Binders—Specifications for Paving Grade Bitumens. BS EN 12591: 2000*. British Standards Institution, London, 2000.
7. British Standards Institution. *Determination of the Indirect Tensile Stiffness Modulus of Bituminous Mixtures. BS 213*. British Standards Institution, London, 1993.
8. British Standards Institution. *Bituminous Mixtures—Test Methods for Hot Mix Asphalt. BS EN 12697: Part 26: Stiffness*. British Standards Institution, London, 2004.
9. European Committee for Standardization. *Bituminous Mixtures—Test Methods for Hot Mix Asphalt. BS EN 12697: Part 24: Resistance to Fatigue*. CEN, Brussels, 2004.
10. Rowe G. M. *Application of the Dissipated Energy Concept to Fatigue Cracking in Asphalt Pavements*. PhD Thesis, University of Nottingham, 1996.
11. European Committee for Standardization. *Bituminous Mixtures—Test Methods for Hot Mix Asphalt, BS EN 12697: Part 35: Laboratory Mixing*. CEN, Brussels, 2002.
12. European Committee for Standardization. *Bituminous Mixtures—Test Methods for Hot Mix Asphalt, BS EN 12697: Part 33: Specimen Prepared by Roller Compactor*. CEN, Brussels, 2003.
13. British Standards Institution. *Bituminous Mixtures—Test Methods for Hot Mix Asphalt. BS EN 12697: Part 6: Determination of Bulk Density of Bituminous Specimens*. British Standards Institution, London, 2002.
14. British Standards Institution. *Bituminous Mixtures—Test Methods for Hot Mix Asphalt. BS EN 12697: Part 5: Determination of the Maximum Density*. British Standards Institution, London, 2002.
15. Di Benedetto H., Ashayer Soltani M. A. and Chaverot P. Fatigue damage for bituminous mixtures: a pertinent approach. *Journal of the Association of Asphalt Paving Technologists*, 1996, **65**, 141–176.
16. Di Benedetto H., de La Roche C., Baaj H., Pronk A. and Lundstrom R. Fatigue of bituminous mixtures. *Materials and Structures*, 2004, **37**, No. 3, 202–216.
17. Pell P. S. and Cooper K. E. The effect of testing and mix variables on the fatigue performance of bituminous materials. *Proceedings of the Association of Asphalt Paving Technologists*, 1975, **44**, 1–37.
18. Van Dijk, W. Practical fatigue characterization of bituminous mixes. *Proceedings of the Association of Asphalt Paving Technologists*, 1975, **44**, 38–82.
19. Van Dijk W. and Visser W. The energy approach to fatigue for pavement design. *Proceedings of the Association of Asphalt Paving Technologists*, 1977, **46**, 1–40.
20. Pronk A. C. and Hopman P. C. Energy dissipation: the leading factor of fatigue. *Proceedings of the Conference on the United States Strategic Highway Research Program*, London, 1991, pp. 255–267.
21. Rowe G. M. Performance of asphalt mixtures in the trapezoidal fatigue test. *Proceedings of Associations of Asphalt Paving Technologists*, 1993, **62**, 344–384.
22. Tayebali A. A., Rowe G. M. and Sousa J. B. Fatigue response of asphalt aggregate mixtures. *Proceedings of Asphalt Paving Technologists*, 1992, **62**, 385–421.
23. Tayebali A. A., Deacon J. A., Coplantz J. S. and Monismith C. L. Modeling fatigue response of asphalt-aggregate mixtures. *Proceedings of Associations of Asphalt Paving Technologists*, 1993, **62**, 385-421.
24. Monismith C. L. *Fatigue Response of Asphalt-aggregate Mixes*. National Research Council, 1994, Washington, DC, USA, SHRP-A-404, Strategic Highway Research Program.
25. Ghuzlan K. A. and Carpenter S. H. Energy-derived, damage failure criterion for fatigue testing. *Transportation Research Record*, 2000, No. 1723, 141–149.
26. Rowe G. M. and Bouldin M. G. Improved techniques to evaluate fatigue resistance of asphaltic mixes. *Proceedings of the Second Euraphalt and Eurobitume Congress*, Barcelona. Foundation Eurasphalt, Breukelen, The Netherlands, 2000, vol. 1, pp. 754–763.
27. Reese R. Properties of aged asphalt binder related to asphalt concrete life. *Journal of the Association of Asphalt Paving Technologists*, 1997, **66**, 604–632.
28. Lee H. J., Kim Y. R. and Lee S. W. *Prediction of Asphalt Mix Fatigue Life with Viscoelastic Material Properties. Transportation Research Record*, No. 1832, 139–147.
29. Kim Y., Lee H. J., Little D. N. and Kim Y. R. A simple testing method to evaluate fatigue fracture and damage performance of asphalt mixtures. *Journal of the Association of Asphalt Paving Technologists*, 2006, **75**, 755–788.
30. Kim Y.-R., Little D. N. and Lytton R. L. Use of dynamic mechanical analysis (DMA) to evaluate the fatigue and healing potential of asphalt binders in sand asphalt mixtures. *Journal of the Association of Asphalt Paving Technologists*, 2002, **71**, 176–206.
31. Wöhler A. Versuche uber die Festigkeit der Eisenbahnwagenachsen, English summary (1867). *Journal of Engineering*, 1860, **4**, 160–161.
32. Pell P. S. Characterisation of fatigue behaviour. *Proceedings of a Symposium on Structural Design of Asphalt Concrete Pavements to Prevent Fatigue Cracking*. National Research Council, Washington, DC, USA, 1973, Highway Research Board, Special Report 140, pp. 49–64.